Int. J. Electrochem. Sci., 11 **(2016)** 3963 - 3975

International Journal of
ELECTROCHEMICAL
SCIENCE
www.electrochemsci.org

Effect of Tin on The Corrosion Resistance of 16 Cr Ferritic Stainless Steel in Acidic Solution and Chloride-Containing Media

Zhenzhen Zhan[1], *Min Sun*[2,3], *Yiming Jiang*[2], *Li Li*[1], *Jin Li*[2]

[1] Analysis and testing center of Fudan University, Shanghai, 200433
[2] Department of Materials Fudan University, Shanghai, 200433
[3] Research Institute, Baoshan Iron & Steel Co., Ltd., Shanghai 201900, PR China
[*]E-mail: corrosion@fudan.edu.cn

Received: 27 January 2016 / *Accepted:* 26 February 2016 / *Published:* 1 April 2016

Newly developed 16 Cr ferritic stainless steel (FSS) containing tin, ranging from 0~0.5 wt.%, are resource-efficient, economic steels with good mechanical properties. In this paper, its corrosion behavior was investigated in acidic solution and chloride-containing media through weight loss measurements, potentiodynamic polarization curves and critical pitting corrosion temperature (CPT). The morphologies of the specimens were studied by scanning electron microscope-energy-dispersive X-ray spectroscopy (SEM-EDS) techniques. Based on the results, the effects of tin element on the corrosion resistance for 16 Cr FSS in different solutions were complex. It could be concluded that the corrosion behaviors of 16 Cr FSS was affected by a small addition of tin in two ways: 1) A SnO_2 layer could be formed over the surface of the specimens and protect them from corrosion, which was then verified by the X-ray photoelectron spectroscopy (XPS); 2) The hydrolysis reaction of Sn^{2+} and Sn^{4+} led to an increase of local concentration of hydrogen ions, which further aggravated the corrosion of the specimens. The whole corrosion resistance of 16 Cr FSS was depended on the two antagonism effects.

Keywords: Tin, 16 Cr Ferritic stainless steel, Corrosion resistance, Pitting corrosion

1. INTRODUCTION

The corrosion resistance of stainless steels is highly dependent on the addition of high-performance alloying elements, like chromium, nickel and molybdenum [1-3]. However, because of small quantity and high price of raw materials, economic stainless steels have drawn lots of attention in

doi: 10.20964/110414

steels industry and research [4-5]. Ferritic stainless steel (FSS) are gradually instead of expensive austenitic stainless steel (ASS) as the first choice in the field of transportation, construction, household appliances and kitchen facilities, etc. because of its good combination properties of low thermal expansion rate, high temperature oxidation resistance, thermal conductivity and no stress corrosion tendency, especially the advantage of resource-saving and price [6-7]. The addition of small amount of alloying element to low Cr-Ni steels, such as Sb, Cu, Si and Sn, can promoted the formation of an oxide and protective layer on the surface and contribute to corrosion resistance of steels. Some researchers have reported that these elements can prevent anodic dissolution of stainless steels in chemically aggressive environments. For example, copper-bearing stainless steels could increase passivation capability and help to improve low-cost steels' corrosion resistance in corrosive solution [8]. The sintering behavior of iron powder compacts containing silicon powder showed that its sinter ability of 304L was markedly improved including sintered density, mechanical properties, corrosion resistance and high temperature oxidation resistance [9]. The addition of antimony and tin in steels also enhanced the corrosion resistance via the continuous oxide layer on the surface inhibiting the corrosion further [10-11].

With respect to the influence of tin addition on the corrosion behavior of stainless steels, only a few references can be found. Pardo et al. studied tin and cooper addition on the corrosion behavior of ASS in sulphuric acid and chloride-containing solutions [12-13]. They found significantly positive effects on pitting corrosion and general corrosion of ASS by reason of friendly Cu-Sn synergy compared to addition increasing Cu or Sn concentration singly. Nam et al. reported the corrosion rate of low-alloy steel decreased with increasing tin content by the formation of a protective SnO_2 layer on the surface which inhibited steel dissolution [14]. At the same time the increase of the iron oxyhydroxides could be resulted from the addition of tin. Meanwhile, the iron oxyhydroxides would form a continuous, adherent rust layer. The stability of the layer could be improved by the interaction of tin with copper and antimony, which might suppress the anodic dissolution of steels. Similarly, El-Sayed et al. revealed the addition of small amount of tin improved corrosion resistance of Sb-Sn alloy because of existence of tin in antimony passivation film and confirmed that the uniform of rust inhibited the ingress of aggressive solution [15]. Aforementioned results showed that tin was regarded as a promising alloying element due to its beneficial effect on improving corrosion behavior of stainless steel and expected to replace the expensive elements in alloy, such as nickel. However, tin might have negative effect on corrosion performance of steels. Wang found optimum amount of tin powder to add was 1.6 wt.% for best corrosion resistance acquired by sintered 304L stainless steels [9]. Pardo et al. also reported the tin addition with limit content larger than 0.1wt.% would inhibit pits nucleation but favor its grows [12-13]. Hence, the addition of tin might have the trends of two antagonism effects on the corrosion resistance of stainless steels.

Based on these findings, tin addition indeed showed good combination with other elements, such as Cu and Sb, and increased corrosion resistance on ASS and low alloy steel. Nevertheless, papers concerning the influence of tin addition on FSS were limited. The effects of tin addition on FSS also needed to be examined. In this study, the corrosion behavior of newly developed economic 16 Cr FSS containing tin, ranging from 0~0.5 wt.%, was investigated in acidic solution and chloride-containing media through weight loss measurements, potentiodynamic polarization curves and critical

pitting corrosion temperature (CPT). The morphologies of the specimens were studied by scanning electron microscope-energy-dispersive X-ray spectroscopy (SEM-EDS) techniques. The surface of corroded sample was characterized by X-ray photoelectron spectroscopy (XPS).

2. EXPERIMENTAL PROCEDURE

The test materials were 16 Cr FSS with different concentrations of tin. Their chemical compositions were given in Tables 1. The samples for weight loss measurements were finished with the size of 3 cm × 2 cm × 0.07 cm by wire-electrode cutting and grounded from 180 to 600 grit gradually. The working area for immersion tests was 3 cm × 2 cm. The samples for other corrosive tests were all in the size of 1 cm × 1 cm which exactly was working area. They were grounded to 2000 grit and polished by 1.5 μm aluminum trioxide polishing paste. All the samples were cleaned in an ultrasonic cleaner with absolute ethyl alcohol and deionized water, then dried and prepared for measurements.

Table 1. Chemical compositions of specimens (wt.%)

Samples	C	Si	Mn	Cr	Nb	N	Ti	Sn
0 Sn	0.010	0.30	0.20	16.30	0.20	0.010	0.080	—
0.1 Sn	0.005	0.31	0.23	16.60	0.20	0.007	0.072	0.101
0.3 Sn	0.009	0.35	0.23	16.57	0.20	0.008	0.084	0.282
0.5 Sn	0.005	0.34	0.24	16.15	0.21	0.0077	0.070	0.473

Tests for weight loss immersions were carried out in 4 wt.% acetic acid and 0.07 M hydrochloric acid, referring to GB-9684-2011 [16] and EN71-3 [17], respectively. The immersion tests in acetic acid were going on in boiling solution for 24 hours, while tests in hydrochloric acid were at 37 °C for 6 hours. After tests, all samples were cleaned with 10 wt.% nitric acid solution at 60 °C for 20 min. Samples were weighted after 48-hour hot drying for. All the tests were repeated with three times to guarantee the reliability of the results.

Potentiodynamic polarization curves and CPT measurements were performed on CHI-660D in the three-electrode system, in which the saturated calomel electrode (SCE) were used as reference electrode, the platinum sheet as a counter electrode and the test material as a working electrode. Potentiodynamic polarization curves were carried out in 0.5 wt.% sodium chloride solution at 50 °C with a scan rate of 0.1667 mV/s from -0.5 to 0.6 V (vs SCE). The potential was defined as pitting corrosion potential (E_b) when current density achieved 1×10^{-4} A/cm^2. The CPT was defined as the temperature at which the current density sharply increased to 1×10^{-4} A/cm^2. CPT measurements were carried out in 1 M sodium chloride solution at an applied potential + 200 mV_{SCE} and with continuously

increased electrolyte temperature at a rate of 1 °C/min until stable pitting occurred. During all the process, pure nitrogen gas was flowed to get rid of oxygen gas.

The morphologies of specimens and microstructures of precipitates were studied by SEM-EDS techniques (SEM, Phillips XL30 FEG). The corrosion products of 0.5 Sn after a 2-hour potentiostatic test in 0.5 wt.% sodium chloride solution at 50 °C were analyzed by XPS (XPS, PHI5300).

3. RESULTS AND DISCUSSION

3.1. Weight-loss tests in 4 wt.% acetic acid solution

Table 2 showed the corrosion rates of 16 Cr FSS with different tin content in 4 wt.% HAc with boiling temperature. The corrosion rates of 0 Sn, 0.1 Sn, 0.3 Sn and 0.5 Sn were 6.33×10^{-3} g/m^2×h, 34.42×10^{-1}, 15.50×10^{-1} and 5.37×10^{-3} g/m^2×h, respectively. It was found that addition of 0.1 wt.% tin inversely accelerated the corrosion rate of 16 Cr FSS in diluted HAc. While with the addition of tin content from 0.1 to 0.5 wt.%, it dramatically reduced the corrosion rates of 16 Cr FSS containing tin in acetic acid. The corrosion rate of 0.5 Sn was even a little lower than the corrosion rate of 0 Sn. These results were not completely in accordance with previous works [14, 18-19]. Nam et al. reported that the corrosion rate of low alloy steel was decreased with increasing tin content from 0 to 0.1 wt.% in an acid chloride solution [14]. Comparing results, the impact of tin addition on corrosion resistance of 16Cr FSS was in doubt. In this and previous work, it could be deduced that tin addition of 16 Cr FSS affected in two ways, protecting matrix from aggressive solution, and accelerating corrosion. Then final corrosion behavior of four samples was related to these two effects and would be discussed later.

Table 2. Result of weight loss measurements in 4 wt.% acetic acid solution at boiling state for 24 h

Samples	*Corrosion Rate* (g/m^2×h)			*Mean*
0 Sn	6.40×10^{-3}	7.24×10^{-3}	5.35×10^{-3}	6.33×10^{-3}
0.1 Sn	42.21×10^{-1}	17.79×10^{-1}	43.27×10^{-1}	34.42×10^{-1}
0.3 Sn	11.52×10^{-1}	0.61×10^{-1}	34.64×10^{-1}	15.50×10^{-1}
0.5 Sn	5.38×10^{-3}	6.02×10^{-3}	4.73×10^{-3}	5.37×10^{-3}

Morphologies of cleaned samples were characterized by scanning electron micrographs, as shown in Figure 1. The variation tend of corrosion behavior was in good agreement with the variation of corrosion rate values. Figure 1(a) showed that there was no general corrosion or obvious localized corrosion occurred in 16 Cr FSS without tin addition. Large amounts of corrosion pits of 0.1 Sn was observed in 0.1 Sn, as shown in Figure 1(b). The pits were mostly contiguous and the diameter of most pits was larger than 10 μm. Comparing Figure 1(b), 1(c) and 1(d), the number of corrosion pits were dramatically decreased with tin content increasing from 0.1 to 0.5 wt.%. The size of most pits was distinctly decreased in 0.3 Sn and there was also no general corrosion or obvious localized corrosion

that occurred in 0.5 Sn. Regular precipitations were observed in the matrix, mainly found in 0.1 Sn and 0.3 Sn, as shown in Figure 1(e) and (f). Then Ti and N peaks were detected by EDS analysis as indicated in Figure 2. The analysis on the 0.3 Sn specimen revealed that the TiN precipitated in the matrix and the zone around TiN existed was easily eroded in acetic acid solution. Kim researched that Ti-stabilized FSS containing low N and C could form cubic TiN or fine TiC precipitations in production process [20-21]. Then Kim et al. reported that the area around these precipitations also could induce Cr segregation which further created surrounded Cr depletion zone and then incomplete passive film on the surface [22-23]. Thus the observed corrosion pits were mainly caused by damaged passive film induced by Cr depletion zone around TiN due to Cr-segregation mechanism. The advantage of tin addition on corrosion resistance of 16 Cr FSS was limited, because the effect of chromium could not be completely replaced by the benefit of tin to form complete passive film.

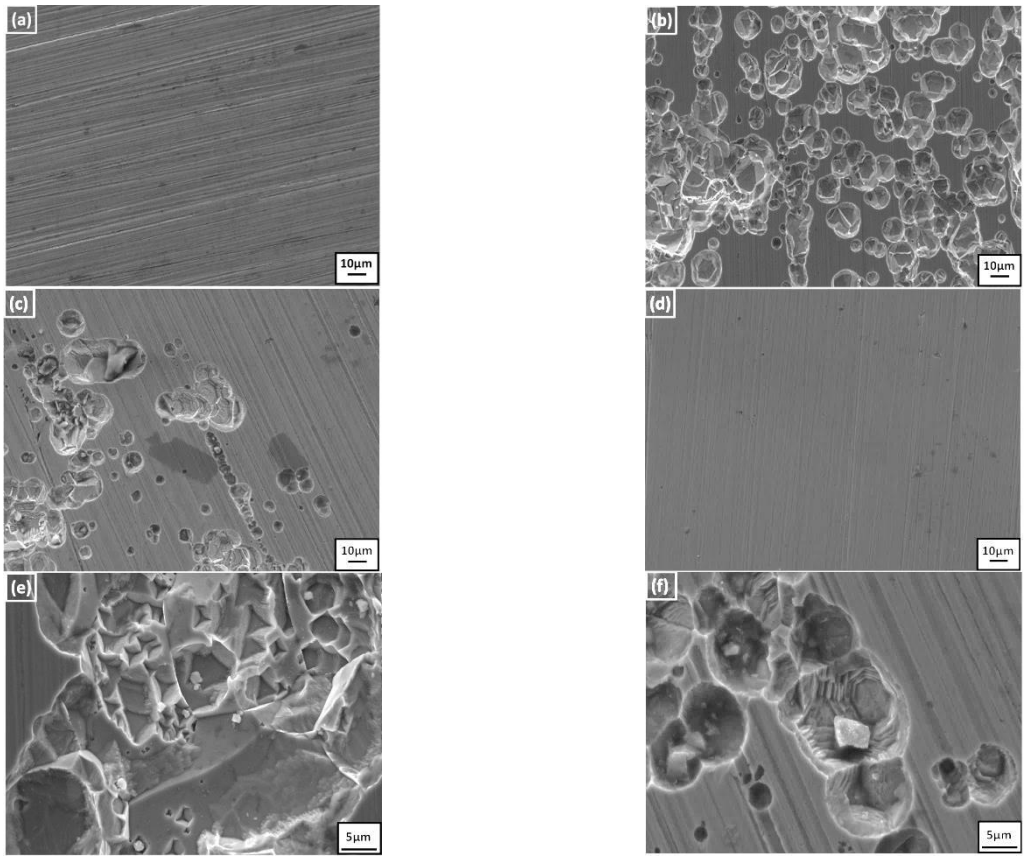

Figure 1. Morphologies of samples with different content of tin after immersed in 4 wt.% HAc solution at boiling state for 24 h: (a) 0 Sn (b) 0.1 Sn (c) 0.3 Sn (d) 0.5 Sn, high resolution (e) 0.1 Sn (f) 0.3 Sn

In mild acid media, the chemical process of 16 Cr FSS containing tin could be possibly described as following equations.

$$Sn - 2e \rightarrow Sn^{2+} \quad (1)$$

$$Sn^{2+} - 2e \rightarrow Sn^{4+} \quad (2)$$

$$2H^{+} + 2e \rightarrow H_2 \quad (3)$$

$$HAc \rightleftarrows H^{+} + Ac^{-} \quad (4)$$

$$Sn^{2+} + 2H_2O \rightarrow Sn(OH)_2 + 2H^{+} \quad (5)$$

$$Sn^{4+} + 2H_2O \rightarrow Sn(OH)_4 + 2H^{+} \quad (6)$$

$$Sn(OH)_4 \rightarrow SnO_2 + 2H_2O \quad (7)$$

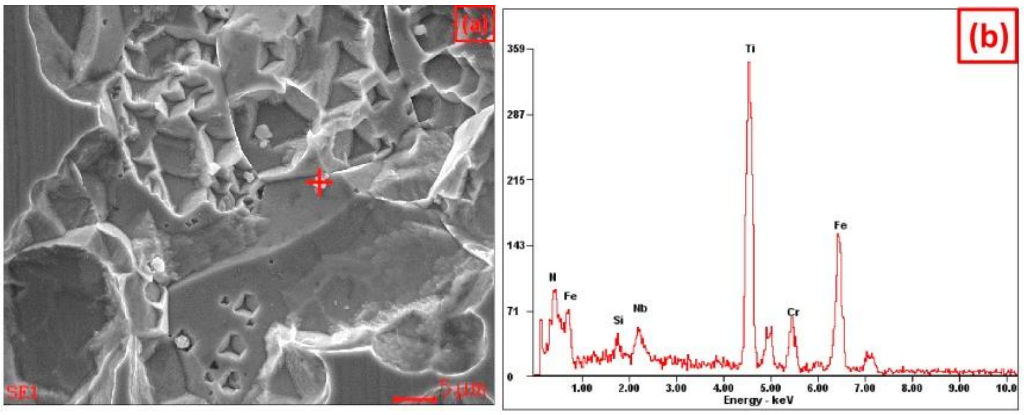

Figure 2. EDS of precipitate in 0.1Sn: (a)marked precipitate (b)EDS spectra of the marked precipitate

The electrochemical reactions on the surface of immersed stainless steels were Eqs. (1-3). The anodic reactions were mainly metal dissolution, firstly tin dissolution, as Eqs. (1-2). The process of tin reactions could prevent 16 Cr FSS from corroding, which delayed pit nucleation as reported by Pardo et al. [12]. The cathodic reaction was hydrogen reduction in acetic acid, as Eq.(3). Eq. (4), a reversible reaction, revealed primary source of hydrogen ion. The ionization constant of acetic acid was 2.37×10^{-4} under boiling condition and the concentration of hydrogen ion was nearly 0.013 M after calculation. Hydrolysis of Sn^{2+} and Sn^{4+}, as Eqs. (5-6), also produced hydrogen ion, which would increase local concentration of hydrogen ion on sample's surface. Therefore, it intensified the cathodic reaction, and anodic reaction followed, as a result, more metal dissolved even iron in matrix. But the formed SnO_2 on the surface of sample produced in hydrolysis improved corrosion resistance of 16 Cr FSS. The formation of tin oxide was described in Eq. (7). Herein, the final corrosion behavior of 16 Cr FSS was depended on combination of two competitive ways after tin addition.

3.2. Weight-loss tests in 0.07 M hydrochloric acid solution

Table 3 showed the variation of the corrosion rate with increasing tin content in 0.07 M HCl at 37 ℃ for 16 Cr FSS. The corrosion rate was 11.92 g/(m^2·h) for the steel without tin addition, and it decreased dramatically to 1.72 g/(m^2·h) when 0.1 wt.% tin was added to 16 Cr FSS. With further increase of tin content, the corrosion rate of samples continuously decreased. Under this condition, there was no doubt that a little suggestion tin addition into 16 Cr FSS could significantly improve the corrosion resistance. The improvement of corrosion resistance was gradually limited by the means of further tin addition. While, the results in hydrochloric acid immersion test were very different from those in acetic acid solution. It would be discussed when analyzing its electrochemical process.

Table 3. Results of weight loss measurements in 0.07 M hydrochloric acid solution at 37 °C for 6 h

Samples	*Corrosion Rate*			*Mean*
	($g/m^2 \times h$)			
0 Sn	12.76	11.71	11.27	11.92
0.1 Sn	1.86	1.81	1.49	1.72
0.3 Sn	1.39	1.48	1.44	1.43
0.5 Sn	1.30	1.33	1.25	1.29

Figure 3 showed the SEM morphologies of specimens after immersion in 0.07 M HCl. The surface of 0 Sn was severely corroded as shown in Figure 3(a). However, the following 16 Cr FSS containing tin were slightly etched as displayed in Figure 3(b-d). Furthermore, the eroding grain boundary was orderly to be mitigated with increasing tin addition into 16 Cr FSS. It was reported that the Cr depletion zone around grain boundary was eroded easily in hydrochloric acid environment [24-25]. The grain boundary was natural barrier for chromium diffusion in production procedure or heat treatment process. Regular TiN precipitation was also found in the grain boundary and on the matrix as shown in Figure 4(a) and 4(c), respectively. Figure 4(b) and 4(d) were the corresponding analysis with EDS. It was obvious that the zone around TiN was damaged, but its extent of corrosion was less than that around grain boundary. Thus the weight loss of 16 Cr FSS containing tin was mainly contributed to by the local corrosion around grain boundary in hydrochloric acid solution.

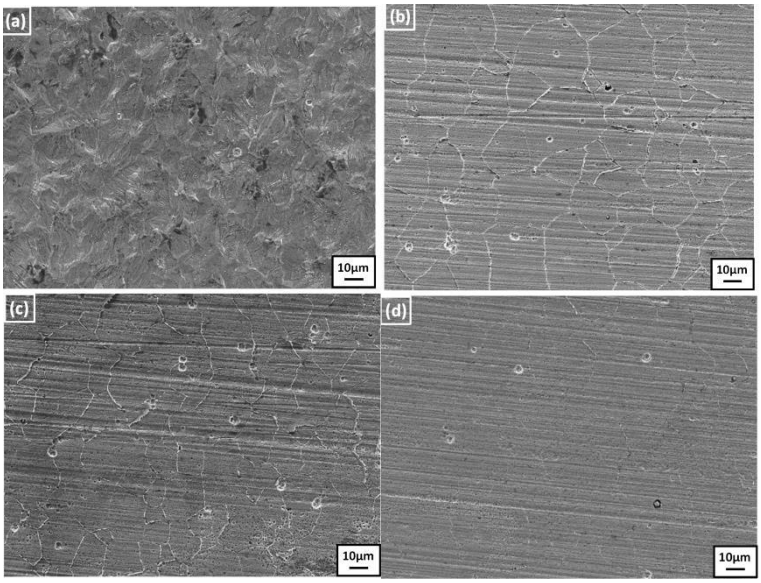

Figure 3. Morphologies of samples with different content of tin after tested in 0.07 M HCl solution at 37 °C for 6 h: (a)0 Sn (b)0.1 Sn (c)0.3 Sn (d)0.5 Sn

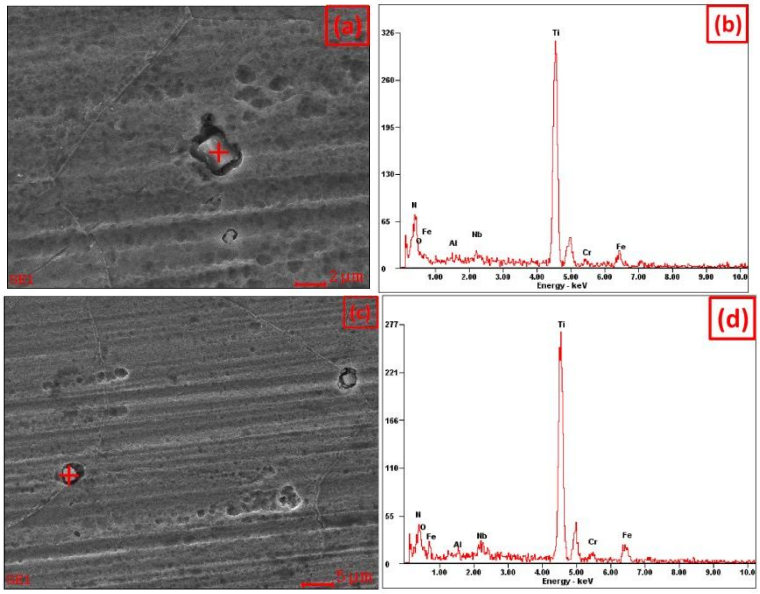

Figure 4. EDS of precipitate in the matrix and grain boundary of 0.1Sn: (a)marked precipitate on the matrix, (b)EDS spectra of the marked precipitate in (a), (c) marked precipitate in the grain boundary, (d)EDS spectra of the marked precipitate in (c)

Hydrochloric acid was strong acid and its electrolytic process was clearly different from acetic acid. Hence the chemical reactions of 16 Cr FSS with tin addition were partly different in hydrochloric acid media. The cathodic and anodic reactions were almost the same as those in acetic acid media. But the hydrogen ion involved in cathodic reaction was from ionization of hydrochloric acid directly, unlike reversible process of electrolytic in acetic acid solution. And the electrolytic process of hydrochloric acid was presented in Eq. (8). Because of the hydrogen ion's complete ionization, its concentration was enough to ignore the effect of hydrogen ion produced by hydrolysis of Sn^{2+} and Sn^{4+}. The beneficial effect of a protective stannic oxide on the surface was more evident than the aggravation of local concentration of hydrogen ion induced by hydrolysis of Sn^{2+} and Sn^{4+}. Therefore, the corrosion rate of specimen 0.1 Sn was slower than that of 0 Sn. And the corrosion resistance of other specimens was also improved with increased tin addition.

$$HCl \rightarrow H^+ + Cl^- \quad (8)$$

3.3. Polarization curve test in neutral sodium chloride media

Figure 5 displayed the typical polarization curves of the samples with different content of tin in 0.5 wt.% sodium chloride solution. During the test, when it applied a certain potential, anodic current density would increase sharply [26-27]. Until current density value reached 1×10^{-4} A/cm^2, the test could be stopped. And the potential now was defined the pitting corrosion potential, E_b. E_{corr} was corrosion potential. The value of (E_b - E_{corr}) could stand for the range of passivation area. To ensure reproducibility, each sample was measured for at least three times. The average values of E_b and E_b –

E_{corr} were showed in Figure 6. Both E_b and $E_b - E_{corr}$ were raised with increasing tin addition of 16 Cr FSS in a way. The results revealed that the pitting corrosion resistance was improved by tin addition, which was possibly caused by enhanced passive film with stannic oxide.

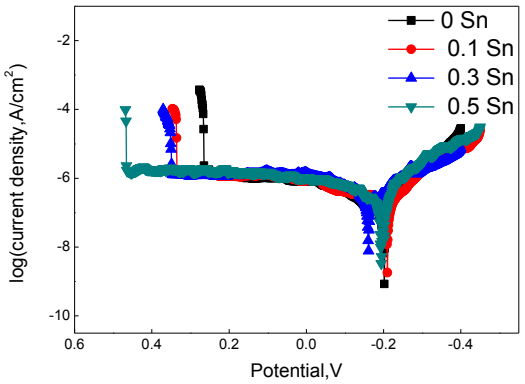

Figure 5. Potentiodynamic polarization curves of the samples with different content of tin in 0.5 wt.% sodium chloride solution at 50 °C

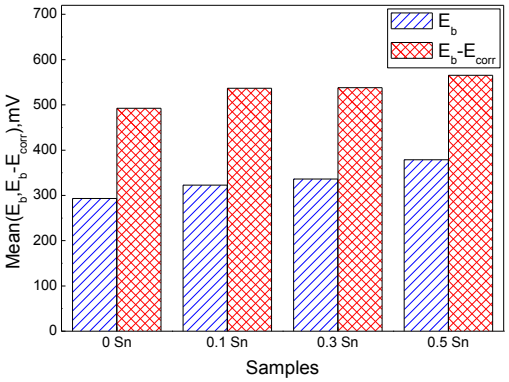

Figure 6. Mean values of E_b and E_b-E_{corr} for samples with different content of tin

3.4. CPT test in neutral sodium chloride media

Figure 7 showed typical curves of current density verses temperature for CPT tests of samples. These measurements in 1 M NaCl were carried out in order to study the influence of tin addition on pitting corrosion resistance of 16 Cr FSS. These results revealed that CPT values were obviously enhanced with increasing tin addition. The current density was in the order of 10^{-6} A/cm^2 before sharp growth, suggesting that the sample was protected well by the formed passive film on the surface. With the solution temperature increasing, further reaching to CPT value, the current density would raise markedly because of the occurrence of stable pit. The CPT value for 0 Sn was 31.5 ℃, while the CPT value for 0.5 Sn were 46.7 ℃. It could be concluded that pitting corrosion resistance of 16 Cr FSS was obviously improved with increasing tin addition. Figure 8 showed the pit morphologies for 0 Sn and 0.5 Sn after CPT tests. The two pictures performed in similar roundness shape with diameter size of about 40 μm.

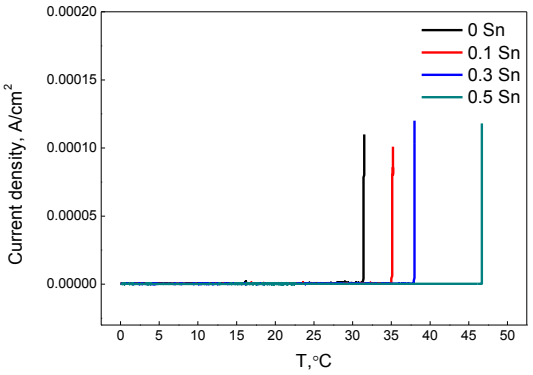

Figure 7. CPT curves of samples with different content of tin in 1 M sodium chloride solution at + 200 mV_{SCE}

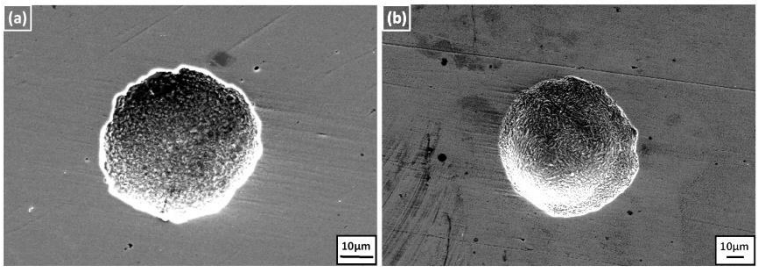

Figure 8. Pitting morphologies of 0Sn and 0.5Sn after CPT test: (a) 0Sn (b) 0.5Sn

The chemical process of 16 Cr FSS containing tin in neutral sodium chloride media was different from the process in acid media. Firstly, cathodic reaction in electrochemical process was another hydrogen reduction, different from that in acid solution as presented in Eq. (9). The produced hydroxyl ion could neutralize the hydrogen ion created by Eqs. (5-6) [28-29]. Secondly, the passive film was mainly damaged by existent chloridion in sodium chloride solution, which caused stable pitting corrosion behavior.

$$2H_2O + 2e \rightarrow 2OH^- + H_2 \qquad (9)$$

3.5. XPS Characterization

The corrosion products on sample surface were characterized by XPS after the potentiostatic test. Figure 9 displayed XPS data for 0.5 Sn including a full range survey and detailed spectra of Fe $2p_{3/2}$, Cr $2p_{3/2}$, and Sn 3d in the passive film. The peaks of O 1s, Fe 2p, Cr 2p and Sn 3d in the full range survey signifying the existence of Cr, Fe, Sn and oxygen on the steel surface. According to reference paper for background removal, the XPS results of Fe $2p_{3/2}$, Cr $2p_{3/2}$, and Sn 3d were separated into dedications for different oxidation state through appropriate procedure explained in previous work. The evaluation of possible species in passive film could be conducted on the basis of

well characterized standards from Handbook of X-ray photoelectron spectroscopy [30], as shown in Table 4.

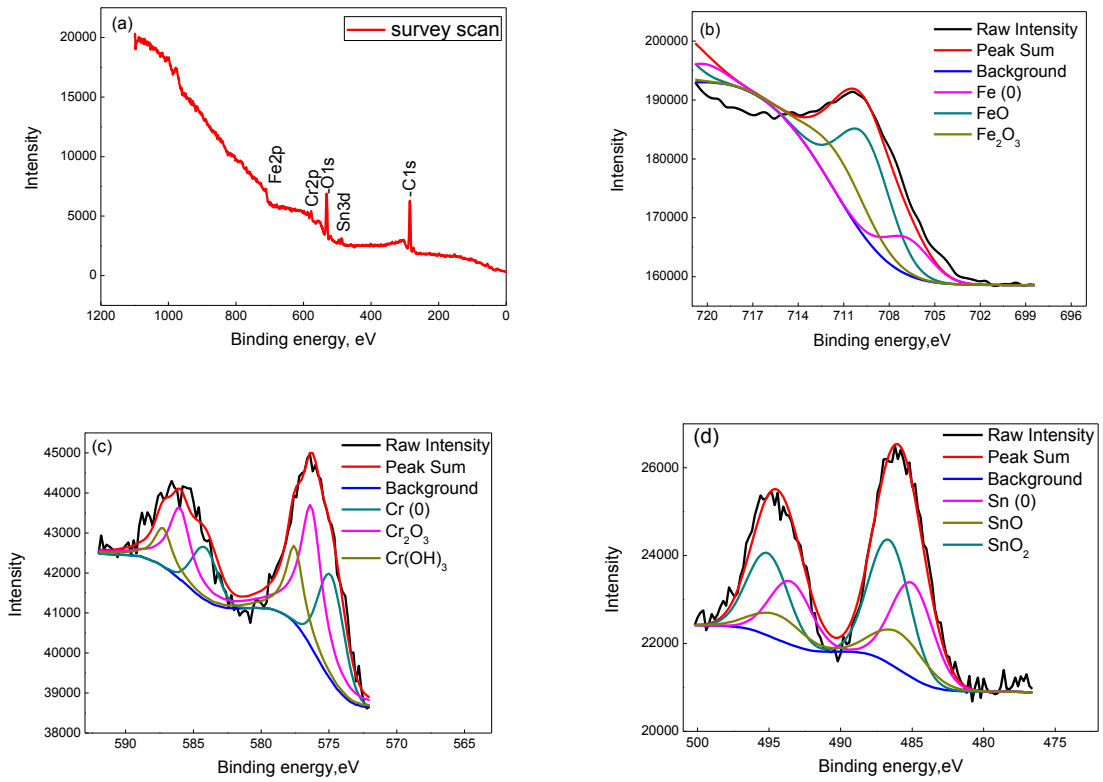

Figure 9. XPS peak analysis for the surface products of 0.5 Sn after potentiostatic test in 0.5 wt.% sodium chloride solution at 50 °C: (a) survey scan spectra and narrow scan spectra of (b)Fe (c)Cr (d)Sn

Table 4. Binding energies (B.E.) of XPS-peaks of standards

Fe $2p_{3/2}$	Peak	Fe (0)	FeO	Fe_2O_3
	B.E.(eV)	706.8	709.6	711.2
Cr $2p_{3/2}$	Peak	Cr (0)	Cr_2O_3	$Cr(OH)_3$
	B.E.(eV)	574.0	576.0	576.4
Sn $3d_{5/2}$	Peak	Sn (0)	SnO	SnO_2
	B.E.(eV)	485.0	485.9	486.6

From the fitting of signals at 0.2 V_{SCE}, the Fe $2p_{3/2}$ spectrum exhibited three main peaks at about 706.8 eV, 709.6 eV, 711.2 eV, which were corresponding to Fe (0), FeO and Fe_2O_3 species, respectively [31-32]. The Cr $2p_{3/2}$ spectrum existed several obvious peaks at about 574.0 eV, 576.0 eV, 576.4 eV, which could be assigned to Cr (0), Cr_2O_3, $Cr(OH)_3$ species, respectively [33-34]. The Sn 3d spectrum displayed three main peaks at about 485.0 eV, 485.9 eV, 486.6 eV, which could be represented as Sn (0), SnO, SnO_2, respectively [35]. These oxidized species are the primary components of the passive film for 16 Cr FSS containing tin in sodium chloride solution.

On the basis of the Pourbaix diagram of Sn/H_2O system and analyzed result by XPS, the formation of SnO_2 in this media was proposed to proceed through Eqs. (5-7) similar to the process in acid media which was described in previous papers [36]. The presence of SnO_2 on the surface of 16 Cr FSS containing tin decreased corrosion rate in acid media due to a decrease in anodic reaction kinetics [14]. Moreover, the passive film enhanced by SnO_2 in neutral chloride media improved local pitting corrosion resistance because of an increase in E_b and CPT. Therefore, the tendency of 16 Cr FSS containing tin to form a SnO_2 oxide layer increased with increasing Sn content.

4. CONCLUSIONS

The effect of tin addition on corrosion resistance of 16 Cr FSS in acid solution and chloride-containing media were investigated. The hydrolysis reaction of Sn^{2+} and Sn^{4+} led to an increase of local concentration of hydrogen ions to aggravate the corrosion of the specimens as one aspect. On the contrary, a protective stannic oxide layer could be formed on the surface, which could further inhibit corrosion in aggressive solutions. Hence, corrosion behaviors of 16 Cr FSS containing tin in different conditions were a combination of two antagonism effects.

(1) In acetic acid solution, the corrosion rates of 0 Sn, 0.1 Sn, 0.3 Sn and 0.5 Sn were first increased when added tin into 16 Cr FSS and then decreased with increasing tin addition.

(2) In hydrochloric acid solution, the corrosion rates of four specimens were obviously decreased with increasing tin addition and the corrosion mainly occurred in grain boundary.

(3) In neutral sodium chloride media, E_b and CPT values of 0 Sn, 0.1 Sn, 0.3 Sn and 0.5 Sn were increased with increasing tin addition, indicating the local pitting corrosion resistance of 16 Cr FSS was improved by tin.

References

1. R. A. Lula, *Stainless steel*, United States: American Society for Metals, 1985.
2. D. Peckner, I. M. Bernstein, *Handbook of stainless steels*, New York: McGraw-Hill, 1977.
3. H. J. Park, H. W. Lee, *Int. J. Electrochem. Sci.*, 9 (2014) 6687.
4. J. Wan, Q. Ran, J. Li, Y. Xu, X. Xiao, H. Yu, L. Jiang., *Mater. Des.*, 53 (2014) 43.
5. S. M. Alvarez, A. Bautista, F. Velasco, *Corros. Sci.*, 53 (2011) 1748.
6. Q. B. Han, E. B. Yue, *Wide and Heavy Plate*, 24 (2005) 4.
7. W. Wu, Y. Guo, H. Yu, Y. Jiang, J Lin, *Int. J. Electrochem. Sci.*, 10 (2015) 10689.
8. N. D. Greene, C. R. Bishop, M. Stern, *J. Electrochem. Soc.*, 108 (1961) 836.
9. W. F. Wang, *J. Mater. Eng. Perform.*, 8 (1999) 649.
10. T. Nishimura, H. Katayama, K. Noda, T. Kodama, *Corros. Sci.*, 42 (2000) 1611.
11. D. P. Le, W. S. Ji, J. G. Kim, K. J. Jeong, S. H. Lee, *Corros. Sci.*, 50 (2008) 1195.
12. A. Pardo, M. C. Merino, M. Carboneras, A. E. Coy, R. Arrabal, *Corros. Sci.*, 49 (2007) 510.
13. A. Pardo, M. C. Merino, M. Carboneras, F. Viejo, R. Arrabal, J. Munoz, *Corros. Sci.*, 48 (2006) 1075.
14. N. D. Nam, M. J. Kim, Y. W. Jang, J. G. Kim, *Corros. Sci.*, 52 (2010) 14.
15. A. E. El-Sayed, A. M. Shaker, H. G. El-Kareem, *Bull. Chem.*, 76 (2003) 1527.
16. GB-9684-2011, *Food safety of Chinese National Standards for stainless steel product*, (2011).

17. EN71-3, *European Standard: Safety of Toys – Part 3: Migration of Certain Elements*, (1994).
18. C. Zhong, F. Liu, Y.T. Wu, J.J. Le, L. Liu, M.F. He, J.C. Zhu, W.B. Hu, *J. Alloy. Compd.*, 520 (20 12) 11.
19. C. Zhong, M.F. He, L. Liu, Y.J. Chen, B. Shen, Y.T. Wu, Y.D. Deng, W.B. Hu, *Surf. Coat. Techno l.*, 205 (2010) 2412.
20. J. K. Kim, B. J. Lee, B. H. Lee, Y. H. Kim, K. Y. Kim, *Scripta. Mater.*, 61 (2009) 1133.
21. J. K. Kim, Y. H. Kim, S. H. Uhm, J. S. Lee, K. Y. Kim, *Corros. Sci.*, 51 (2009) 2716.
22. J. K. Kim, Y. H. Kim, J. S. Lee, K. Y. Kim, *Corros. Sci.*, 52 (2010) 1847.
23. J. K. Kim, Y. H. Kim, B. H. Lee, K. Y. Kim, *Electrochim. Acta*, 56 (2011) 1701.
24. Y. Wang, X. Cheng, X. Li, *Electrochem. Commun.*, 57 (2015) 56.
25. Z. Feng, X. Cheng, C. Dong, L. Xu, X. Li, *Corros. Sci.*, 52 (2010) 3646.
26. J. Liu, W. Hu, C. Zhong, Y.F. Cheng, *J. Power Sources*, 223 (2013) 165.
27. C. Zhong, W.B. Hu, Y.F. Cheng, *J. Power Sources*, 196 (2011) 8064.
28. Z. Y. Liu, X. G. Li, Y. F. Cheng, *Electrochem. Commun.*, (2010) 936.
29. Z. Y. Liu, X. G. Li, Y. F. Cheng, *Electrochim. Acta*, (2012) 259.
30. F. M. John, F. S. William, E. S. Peter, *Handbook of X-ray photoelectron spectroscopy*, Minnesota : Physical Electronics Inc, 1992.
31. M. Finšgar, S. Fassbender, S. Hirth, I. Milosev, *Mater. Chem. Phys.*, 116 (2009) 198.
32. H. Luo, C. F. Dong, X. G. Li, K. Xiao, *Electrochim. Acta.*, 64 (2012) 211.
33. Z. Feng, X. Cheng, C. Dong, L. Xu, X. Li, *Corros. Sci.*, 52 (2010) 3646.
34. H. Li, C. Dong, K. Xiao, X. Li, P Zhong, *Int. J. Electrochem. Sci.*, 10 (2015) 10173.
35. X. Zhong, G. Zhang, Y. Qiu, Z. Chen, X. Guo, C. Fu, *Corros. Sci.*, 66 (2013) 71.
36. C. I. House, G. H. Kelsall, *Electrochim. Acta*, 29 (1984) 1459.